

Binding Interaction of Xanthoxylin with Bovine Serum Albumin

Mao-Gui Wen · Xin-Bo Zhang · Jian-Niao Tian ·
Shou-Hai Ni · He-Dong Bian · Yong-Lin Huang ·
Hong Liang

Received: 15 October 2008 / Accepted: 18 November 2008 / Published online: 12 February 2009
© Springer Science+Business Media, LLC 2009

Abstract Three independent techniques have been used to investigate the interaction between bovine serum albumin (BSA) and xanthoxylin (XT). UV-Vis absorption spectroscopy measurements showed that there is a XT-BSA complex formed with an overall binding constant of $K = 1.01 \times 10^5 \text{ L}\cdot\text{mol}^{-1}$. Spectroscopic techniques including synchronous fluorescence and Fourier transform infrared (FT-IR) were used to assess the structural effects of XT binding on BSA. The FT-IR experiments showed that there is a decrease of the amount of α -helix from 50.2 to 48.1% and an increase of the β -sheet from 32.9 to 36.9% in the XT-BSA complex. In addition, XT binds to site I of the protein with a distance of 2.07 nm between tryptophan residues and XT.

Keywords Bovine serum albumin · Xanthoxylin · Conformational change · Energy transfer

1 Introduction

Xanthoxylin (XT), 2-aceto-3,5-dimethoxyphenol, is a common phenol present in plants of the Rutaceae family that exhibits remarkably potent antioxidation and antibiotic properties

M.-G. Wen · X.-B. Zhang · J.-N. Tian · S.-H. Ni · H. Liang (✉)

Key Laboratory for Chemistry and Molecular Engineering of Medicinal Resources (Guangxi Normal University), Ministry of Education of China, Guilin, Guangxi 54904, China
e-mail: lianghongby@yahoo.com.cn

M.-G. Wen

e-mail: gxnuchem312@yahoo.com.cn

H.-D. Bian (✉)

Chemistry and Chemical Engineering, Guangxi Normal University, Guilin, Guangxi 541004, China
e-mail: bianhd@mailbox.gxnu.edu.cn

Y.-L. Huang

Guangxi Institute of Botany, Guangxi Zhuangzu Autonomous Region and the Chinese Academy of Sciences, Guilin, Guangxi 541004, China

[1, 2]. XT is a natural material that has been used as a heart regent. It has a spontaneous pulsatile effect on cultured mice embryo heart cells [3]. XT and its derivatives have direct inhibition effects on intestinal, uterus and bladder muscle contractions that are caused by some drugs [4]. As a consequence, the study of the binding interaction of xanthoxylin with proteins of biological interest appears to be one of the necessary steps toward a fundamental understanding of the biological activity of these chemicals.

Serum albumin as one of the most abundant carrier proteins plays an important role in the transport and disposition of many drugs in blood [5–7]. Bovine serum albumin (BSA) is well suited to these initial studies since it has been extensively characterized. Many drugs and other small bioactive molecules can bind reversibly to albumins, whereby the latter molecule serves as a carrier. Serum albumins are effective for increasing the solubility of hydrophobic drugs in plasma and modulating their delivery to cells *in vivo* and *in vitro*. Protein-drug interactions play an important role in a variety of biological processes. Studies of this aspect may provide information about structural features that determine the therapeutic effectiveness of drugs, and have become an important research field in life sciences, chemistry, and clinical medicine. Information on the interaction of serum albumin and a particular drug can give rise to a better understanding of the absorption and distribution of that drug. In a previous study using the fluorescence quenching of BSA, we identified an effective interaction between BSA and XT [8]. In order to gain a multidisciplinary insight into the detailed molecular and conformational changes from the XT-BSA interaction, UV-Vis absorption, synchronous fluorescence and infrared spectra bond-resolving technology was used in the present work.

2 Materials and Method

2.1 Materials

Bovine serum albumin was purchased from Sigma. The samples were dissolved in a $0.05 \text{ mol}\cdot\text{L}^{-1}$ phosphate buffer solution (PBS), $\text{pH} = 7.40$, containing $0.1 \text{ mol}\cdot\text{L}^{-1}$ NaCl. All of the chemicals were of high-purity grade and were used without further purification. XT was extracted from *Blumea balsanifera* DC according to the literature method [9]. The $1.5 \times 10^{-3} \text{ mol}\cdot\text{L}^{-1}$ XT stock solution was prepared in ethanol.

2.2 Methods

The UV spectra were recorded on a Cary 100 UV-Visible spectrophotometer (Varian). Quartz cuvettes of 1 cm pathlengths were used. The absorbance titrations were performed by keeping the concentration of BSA constant ($4.0 \times 10^{-6} \text{ mol}\cdot\text{L}^{-1}$) while varying the concentration of XT from 0 to $1.25 \times 10^{-5} \text{ mol}\cdot\text{L}^{-1}$. An equal amount of XT was titrated into the reference cell at the same time. Absorbance titration data were used to determine the binding constant [10]. By assuming that there is only one type of interaction between XT and BSA, Eqs. 1 and 2 are established



$$K = \frac{[\text{BSA} : \text{XT}]}{[\text{BSA}][\text{XT}]} \quad (2)$$

where K is the binding equilibrium constant.

Let $[BSA : XT] = c_B$, then

$$K = \frac{c_B}{(c_{BSA} - c_B) - (c_{XT} - c_B)} \quad (3)$$

where c_{BSA} and c_{XT} are the analytical concentration of BSA and XT in the solution, respectively.

According to the Lambert–Beer law, Eq. 3 can be deduced [11]:

$$\frac{A_0}{A_0 - A} = \frac{\varepsilon_{BSA}}{\varepsilon_B} + \frac{\varepsilon_{BSA}}{\varepsilon_B K c_{XT}} \quad (4)$$

where A_0 and A are the absorbance of BSA at 279 nm in the absence and presence of XT, and ε_{BSA} and ε_B are the molar extinction coefficient of BSA and the bound drug, respectively.

The double reciprocal plot of $1/(A_0 - A)$ versus $1/c_{XT}$ is linear and the binding constant (K) can be estimated from the ratio of the intercept to the slope.

All fluorescence spectra were recorded on a RF-5310PC spectrofluorophotometer (Shimadzu) equipped with a xenon lamp and 1.0 cm quartz cells. Typically, 3 mL of a solution containing an appropriate concentration of BSA was titrated by successive additions of xanthoxin solution. Titrations were performed manually by using micro syringes.

FT-IR spectra were recorded on a Perkin Elmer instrument with a germanium attenuated total reflection (ATR) accessory, a DTGS KBr detector, and a KBr beam splitter ratio. Reference spectra (for exactly the same solution but without the protein) were recorded under identical conditions. Second-derivative spectra were obtained with the derivative function of the original spectra.

3 Results and Discussion

3.1 Binding Studies Using UV Absorption Spectra

UV-Vis absorption studies were performed to ascertain changes of the secondary structure of BSA and to analyze the interaction affinity between XT and BSA. It is well known that the absorption of a chromophore is shifted in directions and magnitudes that depend on whether it is transferred to a more hydrophilic or more hydrophobic environment. These shifts are ascribed to a change of $\pi-\pi^*$ transition brought about by changes in the polarizability of the solvent [12, 13]. There are hypochromicities for both of the absorption bands at 210 and 279 nm (Fig. 1). The hypochromicities and blue shift from 279 to 275 nm indicate that the environment of the tryptophanyl residues of BSA has changed, and the peptide's strand is extended more while the hydrophobicity decreased.

As show in Fig. 1, the absorbance at 279 nm is reduced by 50.1% when the concentration of XT is 1.25×10^{-5} mol·L⁻¹. The data from absorbance titrations were used to construct the plot of $1/(A_0 - A)$ versus $1/(c_{XT})$ (Fig. 2). The double reciprocal plot is linear and gives a binding constant of 1.01×10^5 L·mol⁻¹ for XT-BSA binding.

3.2 Conformation Investigation

The synchronous fluorescence spectra can provide information about the molecular microenvironment in the vicinity of the fluorophore functional groups. It is well known that the fluorescence of BSA comes from the tyrosine, tryptophan, and phenylalanine residues.

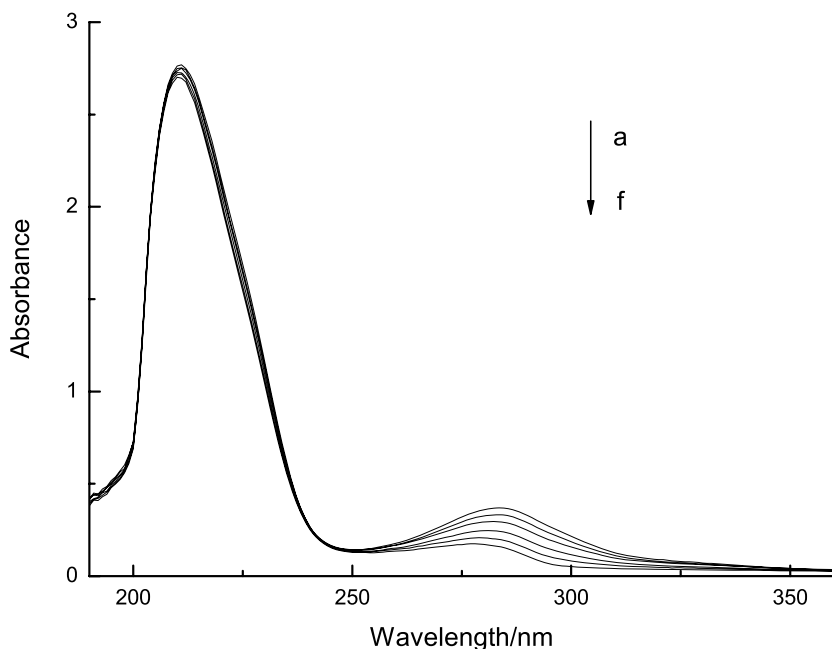


Fig. 1 Absorption spectra of BSA ($4.0 \times 10^{-6} \text{ mol}\cdot\text{L}^{-1}$) in the absence and presence of increasing amounts of XT. From curves *a* to *f*, the concentration of XT was varied from 0 to $1.25 \times 10^{-5} \text{ mol}\cdot\text{L}^{-1}$ at increments of $2.5 \times 10^{-6} \text{ mol}\cdot\text{L}^{-1}$

When the $\Delta\lambda$ values between the excitation and emission wavelengths were stabilized at 15 and 60 nm, the synchronous fluorescence give characteristic information about the tyrosine and tryptophan residues, respectively [10, 14]. The shift in the position of the fluorescence emission maximum corresponds to the changes of the polarity around the chromophore molecule. A blue shift for λ_{max} means that the amino acid residues are located in a more hydrophobic environment, and are less exposed to the solvent, whereas the red shift of λ_{max} implies that the amino acid residues are in a polar environment and are more exposed to the solvent [15–17].

To explore the structural change of BSA from addition of XT, we measured synchronous fluorescence spectra of BSA with various concentrations of XT while the BSA concentration was unchanged. The synchronous fluorescence spectra were measured at $\Delta\lambda = 15 \text{ nm}$ and $\Delta\lambda = 60 \text{ nm}$. As shown in Fig. 3, the effect of XT on the fluorescence intensity of the tyrosine (Fig. 3A) and tryptophan residues (Fig. 3B) of BSA indicated that the main contributions to the fluorescence intensity of BSA resulted from tryptophan residues, because the fluorescence intensity of the tryptophan residues was much stronger than for the tyrosine residues. It is also observed from Fig. 3 that, upon the addition of the XT, there is an obvious red shift of the maximum emission wavelength of the tyrosine residues from 304 to 308 nm (Fig. 3A). On the contrary, a blue shift of the emission maximum of tryptophan residues also occurred from 343 to 341 nm (Fig. 3B), suggesting that the interaction of BSA with XT resulted in a more polar environment for the tyrosine residues, and a more hydrophobic environment for tryptophan residues, which is in agreement with the result of the UV-Vis absorbance spectra. The above conclusions indicate that XT can insert into the BSA molecules and cause molecular conformational changes for BSA.

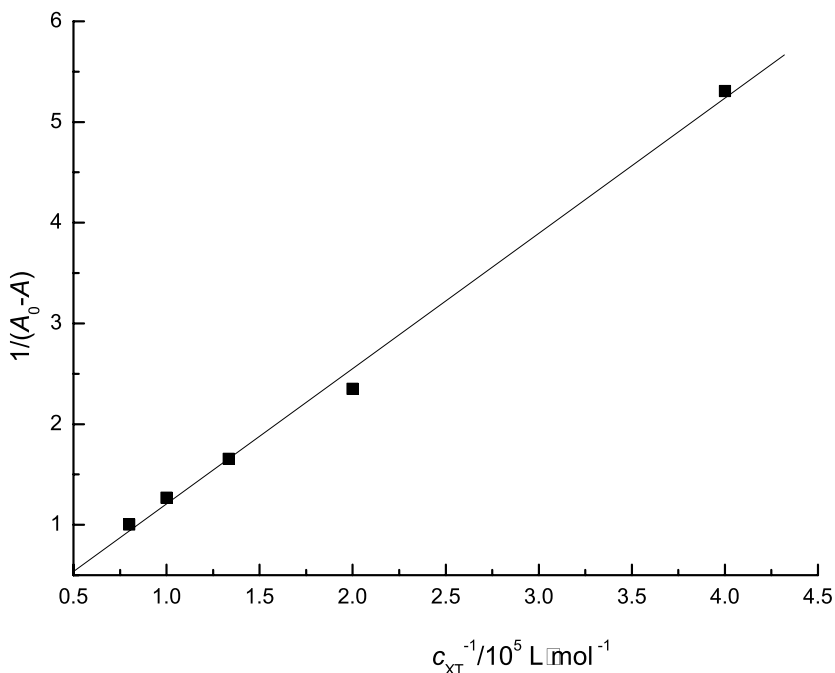


Fig. 2 The plot of $1/(A_0 - A)$ versus $1/c_{XT}$ for BSA-protein and BSA-XT complexes, where A_0 is the initial protein absorption band (279 nm) and A is the recorded absorption at different drug concentrations (c_{XT})

FT-IR spectroscopy offers another valuable method to monitor the changes in the secondary structure of proteins [18]. In our previous research, the FT-IR spectra of XT-BSA showed that the peak position of amide I of BSA moved from 1654 to 1656 cm^{-1} and the peak position of amide II of BSA shifted from 1547 to 1549 cm^{-1} after addition of XT [8]. These results indicate that XT interacts with the C=O and C-N groups in the protein polypeptides. The interaction with XT caused rearrangement of the polypeptide carbonyl hydrogen bonding network and also reduction of the protein α -helical structure. According to the curve-fitted results (Fig. 4), the secondary structure compositions of BSA in the absence and in the presence of XT were estimated. The amount of β -sheet structure composition of BSA increased from 32.9 to 36.9%, the amount of β -turn structure increased from 12.7 to 13.9%, whereas the amount of α -helix structure decreased from 50.2 to 48.1% when the molar concentration ratio of BSA to XT was fixed at 1:1.

3.3 Binding of Fluorescent Probes

The fluorescent probes act as specific markers for distinct binding sites for some drugs on serum albumin. [19] An assay to determine binding sites of XT to BSA was carried out by fluorescence displacement measurements using the following specific probes: ketoprofen for site I [20] and ibuprofen [21] for site II. The percentage of displacement of the probe was determined according to the method of Sudlow et al. [19]

$$\text{probe displacement (\%)} = 10^2 (F_1 / F_2) \quad (5)$$

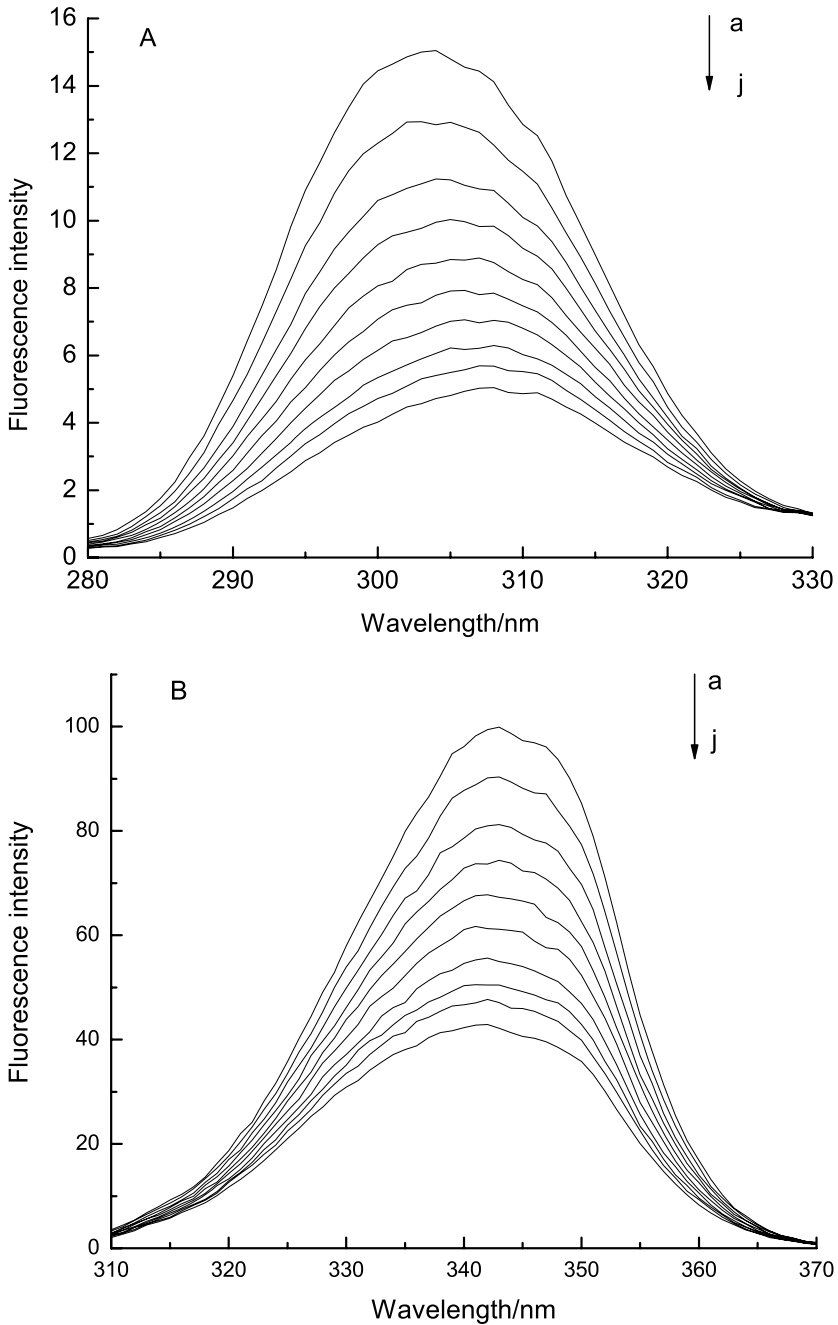


Fig. 3 Synchronous fluorescence spectra of BSA-XT: (A) $\Delta\lambda = 15$ nm; (B) $\Delta\lambda = 60$ nm. The BSA concentration was fixed at 1.0×10^{-5} mol·L $^{-1}$. From *a* to *j*, the concentration of XT was varied from 0 to 4.5×10^{-5} mol·L $^{-1}$ at increments of 5.0×10^{-6} mol·L $^{-1}$

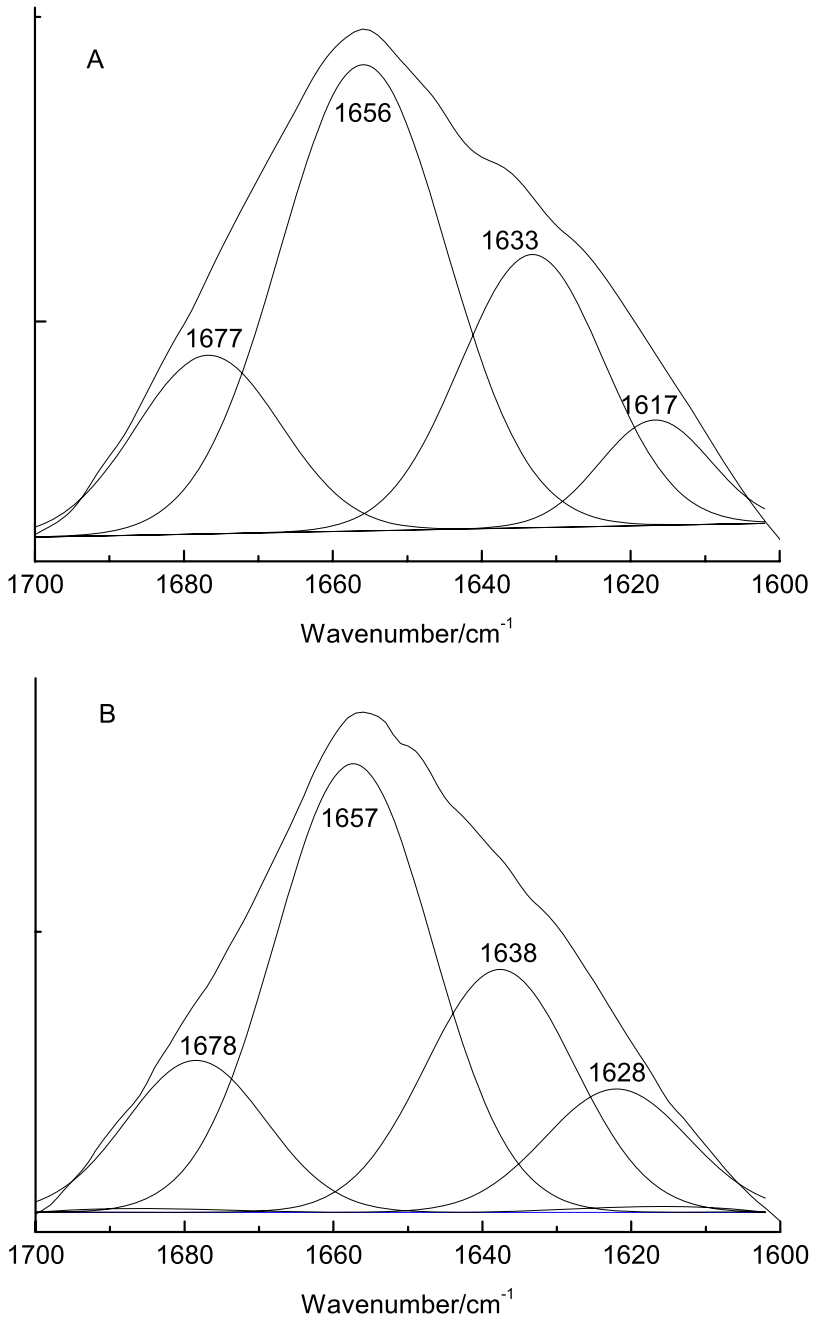


Fig. 4 The curve-fit in the amide I region with secondary structure determination of the free BSA (**A**) and XT-BSA complexes (**B**) in buffer solution in the region of 1600 to 1700 cm⁻¹ (1.0×10^{-3} mol·L⁻¹ BSA; 1.0×10^{-3} mol·L⁻¹ XT) and pH = 7.40

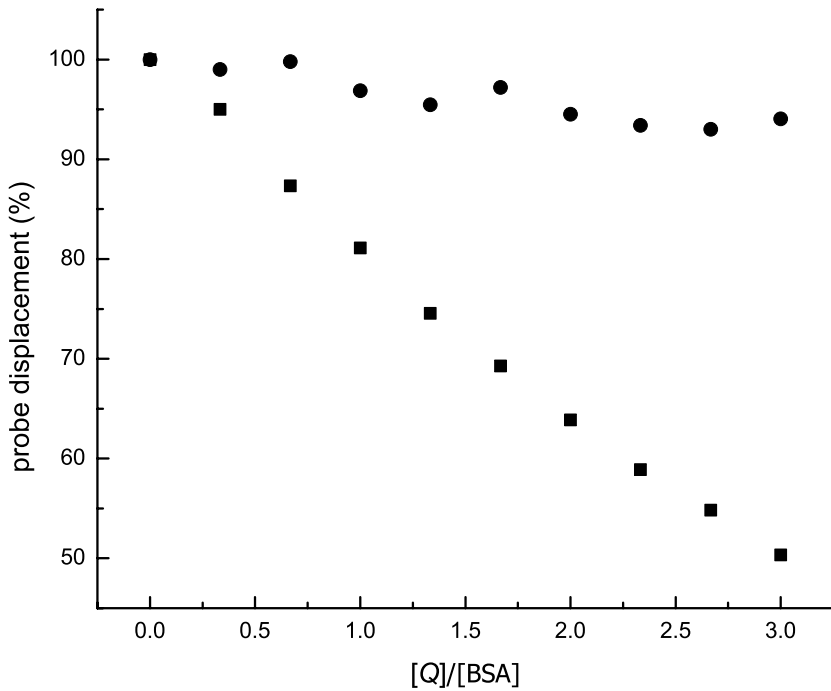


Fig. 5 Effect of the site marker probe on the fluorescence of BSA-XT. The concentrations of BSA and XT were $1.0 \times 10^{-5} \text{ mol}\cdot\text{L}^{-1}$ and $4.0 \times 10^{-5} \text{ mol}\cdot\text{L}^{-1}$, respectively. [Q]: ●, ibuprofen; ■, ketoprofen. pH = 7.40, $\lambda_{\text{ex}} = 280 \text{ nm}$, and $\lambda_{\text{em}} = 344 \text{ nm}$

where F_1 and F_2 denote the fluorescence of XT plus BSA in the absence and presence of the probe, respectively. Figure 5 showed the changes in fluorescence of XT bound to BSA on the addition of the two probes. The relative fluorescence intensity significantly decreased after the addition of ketoprofen but not for ibuprofen, which indicates that XT binds to the site I of BSA.

3.4 Energy Transfer between BSA and XT

The overlap of the UV-Vis absorption spectrum of XT with the fluorescence emission spectrum of BSA is shown in Fig. 6. According to Förster's non-radiative energy-transfer theory [22], the distance between the protein residue (donor) and the bound drug (acceptor) can be calculated by Eq. 6 [23]:

$$E = 1 - \frac{F}{F_0} = \frac{R_0^6}{R_0^6 + r^6} \quad (6)$$

where E is the efficiency of energy transfer between the donor and acceptor, and R_0 is related to the properties of the donor and was calculated by the following equation

$$R_0^6 = 8.8 \times 10^{-25} K^2 n^{-4} \Phi J \quad (7)$$

where K is the orientation factor related to the geometry of the donor and acceptor and K^2 is the spatial orientation factor of the dipole, n is the refractive index of the medium, Φ is

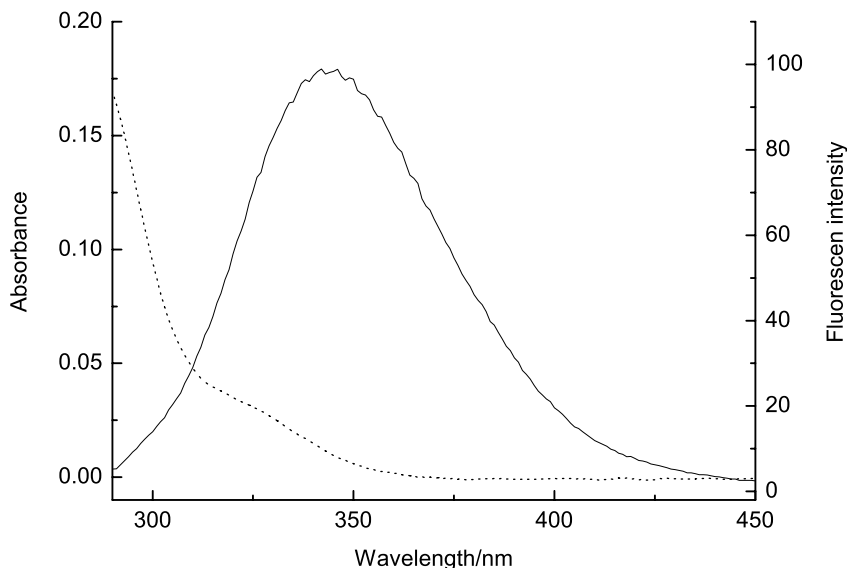


Fig. 6 Spectral overlap between the absorption of XT (1.0×10^{-5} mol·L $^{-1}$) and the normalized emission of BSA (1.0×10^{-5} mol·L $^{-1}$). The solid line is the emission of BSA; the dashed line is the absorption of XT (1.0×10^{-5} mol·L $^{-1}$)

the fluorescence quantum yield of the donor and J is the overlap integral of the fluorescence emission spectrum of the donor and the absorption spectrum of the acceptor. The quantity J is given by Eq. 8,

$$J = \frac{\sum F(\lambda)\varepsilon(\lambda)\lambda^4\Delta\lambda}{\sum F(\lambda)\Delta\lambda} \quad (8)$$

where $F(\lambda)$ is the fluorescence intensity of the fluorescence donor at wavelength λ and ε is the molar absorption coefficient of the acceptor at wavelength λ . In the present case, $K^2 = 2/3$, $n = 1.36$, and $\Phi = 0.15$ [24]. From the data of XT, R_0 was calculated to be 1.67 nm, leading to an estimate of $r = 2.07$ nm, the apparent distance between Trp-214 in site I and the XT. The absolute value of the average distance r between the donor fluorophore and the acceptor in the 2 to 8 nm range, and the fulfillment of the required condition $0.5R_0 < r < 1.5R_0$, converge to indicate that energy transfer from BSA to XT occurs with high probability [25].

4 Conclusions

Under simulated physiological conditions (pH = 7.40, ionic strength 0.10 mol·L $^{-1}$) *in vitro*, we determined the main interaction of BSA with XT by UV-Vis absorbance spectra, FT-IR and synchronous fluorescence spectra methods. The FT-IR results show that changes of the microenvironment of BSA are induced by the binding of XT, with the amount of α -helix structure decreased and the amount of β -sheet structure increased. Furthermore, according to Förster's non-radiative energy-transfer theory, energy transfer from BSA to XT occurs with high probability.

Acknowledgements This work was supported by the National Natural Science Foundation of China (No. 20671023), the Science Foundation of Guangxi Province, the foundation of Key Laboratory for Chemistry and Molecular Engineering of Medicinal Resources (Guangxi Normal University), the Ministry of Education of China and the Innovation Project of Guangxi Graduate Education (No. 2008106020703M251).

References

1. Roesler, R., Catharino, R.R., Malta, L.G., Eberlin, M.N., Pastore, G.: Antioxidant activity of *Annona crassiflora*: characterization of major components by electrospray ionization mass spectrometry. *Food Chem.* **104**, 1048–1054 (2007). doi:[10.1016/j.foodchem.2007.01.017](https://doi.org/10.1016/j.foodchem.2007.01.017)
2. Van der Schyve, C.J., Dekker, T.G., Snyckers, F.O.: Synthesis and antimicrobial activity of a series of caespitin derivatives. *Antimicrob. Agents Chemother.* **30**, 375–381 (1986)
3. Huang, X.-L., Kakiuchi, N., Che, Q.-M., Huang, S.-L., Hattori, M., Namba, T.: Effects of extracts of *Zanthoxylum* fruit and their constituents on spontaneous beating rate of myocardial cell sheets in culture. *Phytother. Res.* **7**, 41–48 (1993)
4. Calixto, J.B., Miguel, O.G., Yunes, R.A., Rae, G.A.: Action of 2-hydroxy-4, 6-dimethoxy aceoephone isolated from *Sebastiania schottiana*. *Planta Med.* **56**, 31–35 (1990). doi:[10.1055/s-2006-960878](https://doi.org/10.1055/s-2006-960878)
5. Carter, D., Ho, J.X.: Structure of serum albumin. *Adv. Protein Chem.* **45**, 153–203 (1994). doi:[10.1016/S0065-3233\(08\)60640-3](https://doi.org/10.1016/S0065-3233(08)60640-3)
6. Sulkowska, A.: Interaction of drugs with bovine and human serum albumin. *J. Mol. Struct.* **614**, 227–232 (2002). doi:[10.1016/S0022-2860\(02\)00256-9](https://doi.org/10.1016/S0022-2860(02)00256-9)
7. Hu, Y.-J., Liu, Y., Pi, Z.-B., Qu, S.-S.: Interaction of cromolyn sodium with human serum albumin: A fluorescence quenching study. *Bioorg. Med. Chem.* **13**, 6609–6614 (2005). doi:[10.1016/j.bmc.2005.07.039](https://doi.org/10.1016/j.bmc.2005.07.039)
8. Wen, M.-G., Tian, J.-N., Huang, Y.-L., Bian, H.-D., Chen, Z.-F., Liang, H.: Interaction between xanthoxylin and bovine serum albumin. *Chin. J. Chem.* **27**, 227–234 (2009)
9. Zhu, T.-C., Wen, Y.-X., Wang, H.-S., Huang, Y.-L.: Study on the chemical constituents of blumea (I). *Guihaia* **28**, 139–141 (2007)
10. Abert, W.C., Gregory, W.M., Allan, G.S.: The interaction of coomassie blue with proteins. *Anal. Biochem.* **213**, 407–413 (1993). doi:[10.1006/abio.1993.1439](https://doi.org/10.1006/abio.1993.1439)
11. Polet, H., Steinhardt, J.: Binding-induced alterations in ultraviolet absorption of native serum albumin. *Biochemistry* **7**, 1348–1356 (1968). doi:[10.1021/bi00844a015](https://doi.org/10.1021/bi00844a015)
12. Zhong, W.-Y., Wang, Y.-C., Yu, J.-S., Liang, Y.-Q., Ni, K.-Y., Tu, S.-Z.: The interaction of human serum albumin with a novel antidiabetic agent—SU-118. *Pharm. Sci.* **93**, 1039–1046 (2004). doi:[10.1002/jps.20005](https://doi.org/10.1002/jps.20005)
13. Shahid, F., Gomez, J.E.: The lanthanide-induced NF transition and acid expansion of serum albumin. *J. Biol. Chem.* **257**, 5618–5622 (1982)
14. Miller, J.N.: Recent advances in molecular luminescence analysis. *Anal. Proc.* **16**, 203–208 (1979)
15. Chen, G.-Z., Hang, X.-Z., Xu, J.-G., Zheng, Z.-Z., Wang, Z.-B.: *Method of Fluorescence Analysis*, 2nd edn. Science Press, Beijing (1990)
16. Hu, Y.-J., Liu, Y., Wang, J.-B., Xiao, X.-H., Qu, S.-S.: Study of the interaction between monoammonium glycyrrhizinate and bovine serum albumin. *J. Pharm. Biomed. Anal.* **36**, 915–919 (2004). doi:[10.1016/j.jpba.2004.08.021](https://doi.org/10.1016/j.jpba.2004.08.021)
17. Tan, F., Guo, M., Yu, Q.-S.: Studies on interaction between gatifloxacin and human serum albumin as well as effect of copper (II) on the reaction. *Spectrochim. Acta A, Mol. Biomol. Spectrosc.* **61**, 3006–3012 (2005). doi:[10.1016/j.saa.2004.11.019](https://doi.org/10.1016/j.saa.2004.11.019)
18. Mantsch, H.H., Chapman, D.: *Infrared Spectroscopy of Biomolecules*. Wiley, New York (1996)
19. Sudlow, G., Birkett, D.J., Wade, D.N.: Further characterization of specific drug binding sites on human serum albumin. *Mol. Pharmacol.* **12**, 1052–1061 (1976)
20. Mignot, I., Presle, N., Lopicque, F., Monot, C., Dropsy, R., Netter, P.: Albumin binding sites for etodolac enantiomers. *Chirality* **8**, 271–278 (1996). doi:[10.1002/\(SICI\)1520-636X\(1996\)8:3<271::AID-CHIR7>3.0.CO;2-K](https://doi.org/10.1002/(SICI)1520-636X(1996)8:3<271::AID-CHIR7>3.0.CO;2-K)
21. He, X.-M., Carter, D.C.: Atomic structure and chemistry of human serum albumin. *Nature* **358**, 209–215 (1992). doi:[10.1038/358209a0](https://doi.org/10.1038/358209a0)
22. Förster, T., Sinanoglu, O.: *Modern Quantum Chemistry*. Academic Press, New York (1996), p. 93
23. Il'ichev, Y.V., Perry, J.L., Simon, J.D., Dockal, M.: Interaction of ochratoxin A with human serum albumin: preferential binding of the dianion and pH effects. *J. Phys. Chem. B* **106**, 452–459 (2002). doi:[10.1021/jp012314u](https://doi.org/10.1021/jp012314u)

24. Hu, Y.-J., Liu, Y., Zhao, R.-M., Dong, J.-X., Qu, S.-S.: Interaction of methylene blue with bovine serum albumin. *J. Photochem. Photobiol. A. Chem.* **179**, 324–329 (2006). doi:[10.1016/j.jphotochem.2005.08.037](https://doi.org/10.1016/j.jphotochem.2005.08.037)
25. Weiss, S.: Fluorescence spectroscopy of single biomolecules. *Science* **283**, 1676–1683 (1999). doi:[10.1126/science.283.5408.1676](https://doi.org/10.1126/science.283.5408.1676)